Ferromagnetism in the Fe-substituted spinel semiconductor ZnGa$_2$O$_4$

Ferromagnetism in the Fe-substituted spinel semiconductor ZnGa$_2$O$_4$

T Maitra and Roser Valentí

Institut für Theoretische Physik, J W Goethe Universität, Max-von-Laue-Strasse 1,
60438 Frankfurt am Main, Germany

Abstract
Motivated by the recent experimental observation of long range ferromagnetic
order at a relatively high temperature of 200 K in the Fe-doped ZnGa$_2$O$_4$
semiconducting spinel, we propose a possible mechanism for the observed
ferromagnetism in this system. We show, supported by band-structure
calculations, how a model similar to the double-exchange model can be written
down for this system and calculate the ground state phase diagram for the two
cases where Fe is doped either at the tetrahedral position or at the octahedral
position. We find that in both cases such a model can account for a stable
ferromagnetic phase in a wide range of parameter space. We also argue that in
the limit of high Fe^{2+} concentration at the tetrahedral positions a description in
terms of a two-band model is essential. The two e$_g$ orbitals and the hopping
between them play a crucial role in stabilizing the ferromagnetic phase in this
limit. The case when Fe is doped simultaneously at both the tetrahedral and
the octahedral position is also discussed.

(Some figures in this article are in colour only in the electronic version)

1. Introduction

Diluted magnetic semiconductors (DMSs) are currently being intensively studied in connection
with their possible application for spintronic devices [1]. Special attention has been devoted
to the III–V semiconductors [1, 2] which develop long range ferromagnetic order with Curie
temperatures of about 100 K upon doping with a low concentration of magnetic impurities like
Mn. Since spintronic applications would become widely accessible if ferromagnetism was
achieved at room temperature, there is a continuous search for new materials with high Curie
temperatures.

In a very recent experiment [3], Risbud and co-authors tried to dope Fe into ZnGa$_2$O$_4$
by preparing a solid solution [ZnGa$_2$O$_4$]$_{1-x}$[Fe$_3$O$_4$]$_x$ of ZnGa$_2$O$_4$ and Fe$_3$O$_4$ with $x = 0.05$,
0.10 and 0.15. Long-range magnetic order was observed in all three samples with Curie
temperatures up to 200 K as well as ferromagnetic hysteresis of the magnetization at low

temperatures. Interestingly, the saturation magnetic moment, which should be 4 μ_B per Fe_3O_4 unit, is about 1 μ_B instead. This has been interpreted [3] as an indication of a certain fraction of Fe not contributing to the ferromagnetic long range order (LRO). These authors have also performed Mossbauer experiments in order to ascertain the oxidation states of Fe in the host semiconductor $ZnGa_2O_4$. For an $x = 0.15$ doped sample they observed the presence of only Fe^{3+} states with some of them displaying a paramagnetic signal (doublet) and the rest showing magnetically ordered Fe^{3+}. We note at this point that in the context of Fe_3O_4 it has already been argued that above the Verwey transition [4] an Fe^{2+} cation can be viewed as an Fe^{3+} ion plus a delocalized electron. We deliberate further on this point in section 7.

Motivated by these observations and the difference between this system and the III–V semiconductors, we investigate in what follows the underlying mechanism of the long range ordering of Fe ions in doped $ZnGa_2O_4$ considering various possible limits of the problem in terms of an effective model which is based on the band-structure calculation of the system. The band-structure calculation, which will be discussed in the next section, gives information about the position and nature of the Fe bands and their hybridization with the bands of the parent compound as well as the active bands at the Fermi level, which will help us to construct an effective Hamiltonian for the system. The ground state magnetic phase diagrams of this effective Hamiltonian are then calculated using the parameters derived from the band-structure calculation.

The host semiconductor $ZnGa_2O_4$ has a spinel crystal structure AB_2O_4 with two cation sites: Zn^{2+} (A) in a tetrahedral co-ordination and Ga^{3+} (B) in an octahedral co-ordination of oxygens. Fe_3O_4 has, on the other hand, an inverse spinel structure with a chemical composition $Fe_A^{3+}[Fe^{2+}, Fe^{3+}]_B O_4^{2-}$. When Fe is substituted in $ZnGa_2O_4$ via the solid solution $[ZnGa_2O_4]_{1-x}[Fe_3O_4]_x$, it can either replace Zn in the tetrahedral position or Ga in the octahedral position or both. Here we will consider the following two cases: (i) all substituted Fe are in tetrahedral positions and (ii) all substituted Fe are in octahedral positions. We also assume the most general case, namely, that Fe can have both Fe^{3+} and Fe^{2+} oxidation states irrespective of whether it is in tetrahedral or octahedral position and that it is always in a high spin state with spin $= 5/2$ and 2 respectively[1]. We will briefly outline the case where Fe ions are in both tetrahedral and octahedral positions at the end.

The paper is organized as follows. In section 2 we discuss our band-structure calculations and present the density of states for the case of Fe doped into tetrahedral positions in $ZnGa_2O_4$. Out of these results we get insight about the active orbitals at the Fermi level which are relevant for our model Hamiltonian. In section 3 we investigate three different limits of the case with Fe occupying tetrahedral positions and motivate a model similar to double exchange for this system. In section 4 we present the model Hamiltonian and calculate the magnetic phase diagram. Section 5 deals with the effect of the Coulomb correlation on the phase diagram results. In section 6 we study the case of Fe doping in the octahedral positions and finally in the last section we discuss our results and make a comparison with the experimental observations.

2. Band-structure calculations

$ZnGa_2O_4$ is a direct bandgap semiconductor with an energy gap of about 4.1 eV [5, 6]. Previous band-structure calculations [7] for $ZnGa_2O_4$ showed that the valence states right below the Fermi level are mostly of oxygen character with the contribution of Zn and Ga being very small. In order to investigate the effect of the doping of Fe in the band structure of $ZnGa_2O_4$, we considered modified unit cells of $ZnGa_2O_4$ with different Fe contents, i.e. Fe substituting

---

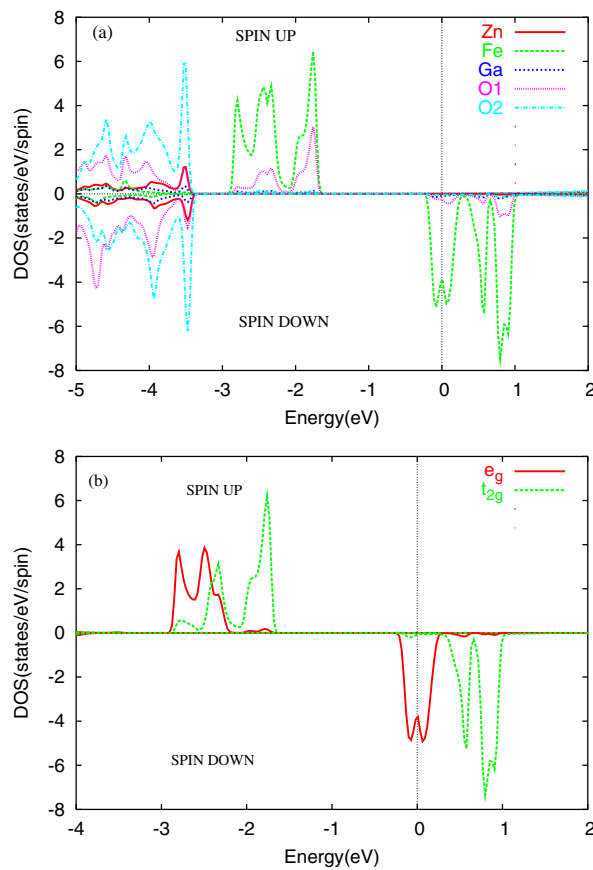[1] In the spinel structure Fe usually acquires the high spin state.

Figure 1. Majority (up) and minority (down) spin density of states for Fe doped into the tetrahedral Zn position in ZnGa$_2$O$_4$. (a) The total density of states and (b) the partial Fe–d density of states as explained in the text. Here O1 and O2 denote two nonequivalent oxygen atoms of the modified unit cell.

Zn in tetrahedral sites in an Fe:Zn ratio 1:2 (50% doping of Fe) and Fe substituting Ga in octahedral sites in an Fe:Ga ratio 1:4 (25% doping of Fe). These percentage dopings of Fe in Zn (or A) sites and in Ga (or B) sites are close to the experimental ones with $x = 0.15$ in the $[\text{ZnGa}_2\text{O}_4]_{1-x}[\text{Fe}_3\text{O}_4]_x$ formula unit which are 45% when Fe substitutes Zn only and 22.5% when Fe substitutes Ga only. Here we will illustrate the tetrahedral substitution.

ZnGa$_2$O$_4$ crystallizes in a normal spinel structure with space group $Fd\bar{3}m$ and the primitive (rhombohedral) unit cell contains two formula units. In order to substitute Fe in one of the Zn positions, one has to make the two Zn positions in the unit cell nonequivalent. One maximal subgroup of $Fd\bar{3}m$ which allows for this substitution is $F\bar{4}3m$. In this new space group we have in addition to Zn, Fe and Ga two nonequivalent oxygen positions O$_1$ and O$_2$. Fe and Zn are surrounded by O$_1$ and O$_2$ ions respectively in a tetrahedral environment, whereas Ga is in an octahedral surrounding with three O$_1$ and three O$_2$ atoms [8].

We have performed *ab initio* density functional theory calculations for Fe doped ZnGa$_2$O$_4$ in the $F\bar{4}3m$ symmetry within the local spin density approximation (LSDA) using the linearized augmented plane waves (LAPWs) as basis set [9]. In figure 1 we present the spin polarized

density of states (DOS) for Fe doped $ZnGa_2O_4$ where Fe substitutes 50% of tetrahedral Zn atoms in the unit cell as described above. Total densities of states of majority (up) and minority (down) spin states for all the atoms are given in figure 1(a) while in figure 1(b) we show the partial density of states for Fe d states projected into t_{2g} and e_g symmetries in both spin directions. We observe that the Fe d states appear to be mainly located in the bandgap of the host semiconductor together with a non-negligible contribution of O_1 p states while Zn, Ga and O_2 contributions are well down into the valence band and are negligible at the Fermi level (figure 1(a)). The Fe DOS shows the expected e_g–t_{2g} splitting for a transition metal ion in a tetrahedral crystal field. The majority spin (spin up) e_g and t_{2g} states are completely filled and appear far below the Fermi level whereas the minority spin (spin down) e_g states are partially filled and are at the Fermi level (figure 1(b)). It is important to note that the spin exchange splitting ($\sim$2.6 eV) is much larger than the crystal field splitting ($\sim$0.5 eV) in this system. These observations of the band structure calculation are crucial to build up an effective model for this system, as we will see below.

3. Model: Fe in tetrahedral position

Based on the electronic structure calculations described above for the doped system, we now motivate a possible mechanism for the ferromagnetic LRO observed in Fe doped $ZnGa_2O_4$. We note at this point that the Fe concentration in this system is *not* very low as for $x = 0.15$ in the $[ZnGa_2O_4]_{1-x}[Fe_3O_4]_x$ formula unit the Fe:Zn ratio calculated from the nominal composition is 1:1.9 ($3x$:$1 - x$) or close to 1:2 though Risbud *et al* reported to have observed a Fe:Zn ratio of 1:3 [3]. Hence the system is not likely to be a candidate for description in terms of a Kondo impurity model [10]. It is rather much more reasonable to assume that the electrons hop between doped sites via mainly the oxygen orbitals in the same way as in the double exchange mechanism in the manganites [11]. We would like to note here that in the case of manganites each Mn ion is surrounded by oxygen atoms in an octahedral environment and these octahedra are corner shared. The double-exchange mechanism then operates through a path of the type Mn–O–Mn giving rise to a ferromagnetic order among the Mn spins. In the present system we observe that for the doping considered in our band structure calculation there exist paths of the type Fe–O_1–O_1–Fe, where O_1 is one of the two nonequivalent oxygens which surrounds Fe in a tetrahedral environment as described in the previous section. This assumption of electron transport via oxygen orbitals is supported by our band-structure calculations, where we see that there exists a small but finite hybridization between the doped Fe and O_1 at the Fermi level (see figure 1(a)). Note that the contribution of Zn, Ga and O_2 is negligible at the Fermi level and hence these are very unlikely to take part in the electronic transport.

A double-exchange-like mechanism mediating ferromagnetism has been proposed and is being seriously investigated lately for various diluted magnetic semiconductors [12–14]. First principles calculations have also been seen to support such a mechanism for ferromagnetic order in some of these systems like ZnO based DMS, Ga(Mn)As [12, 15]. Indeed, without such a long range transport of electrons, the ferromagnetic LRO (long range order) observed in these systems would be difficult to account for, a view shared in other theoretical analyses [16] of LRO in DMS. We would like to emphasize though that the Fe doped $ZnGa_2O_4$ that we are considering here is not strictly a DMS as the doping level is quite high.

Let us consider first the case where all the doped Fe are in tetrahedral positions. In figure 2 we draw a schematic energy level diagram of Fe 3d orbitals together with the valence and conduction bands of the host semiconductor. We discuss in the following three limits of the problem: (i) all or most of the Fe are Fe^{3+}, (ii) Fe is in both Fe^{2+} and Fe^{3+} oxidation states and (iii) the limit of high Fe^{2+} concentration.
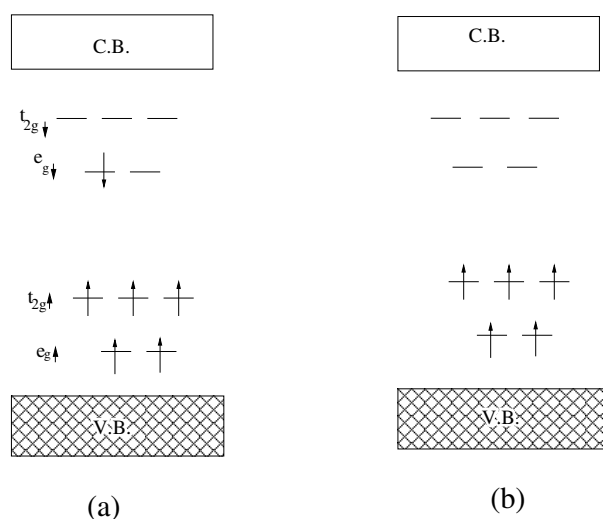
Figure 2. Schematic energy level diagram showing the 3d states of doped Fe in the bandgap of the ZnGa$_2$O$_4$ semiconductor. (a) Fe^{2+} and (b) Fe^{3+} in a tetrahedral crystal field. VB and CB denote the valence band and conduction band of the semiconductor respectively.

3.1. High Fe^{3+} concentration limit

In the situation when neighbouring doped tetrahedral sites are all Fe^{3+}, there are five electrons of the same spin in each site due to Hund's rule. If the spins at these neighbouring doped sites are ferromagnetically aligned then hopping of an electron between sites is blocked by the Pauli principle. If instead they are antiferromagnetically aligned the system gains superexchange energy by a virtual process of electron transfer between the Fe ions. Therefore, when all Fe ions are in an Fe^{3+} state, an antiferromagnetic (AFM) alignment of spins is energetically preferred.

3.2. Mixed Fe^{2+} and Fe^{3+}

Let us examine now the case where both Fe^{2+} and Fe^{3+} are present in neighbouring sites (see figure 3). If the five electrons in Fe^{2+} (all aligned) are in an antiferromagnetic configuration with the spins of the neighbouring Fe^{3+} (figure 3(a)), then an electron in Fe^{2+} has to pay an amount of energy equal to the Hund's coupling (J_H) in order to hop from one Fe^{2+} site to a neighbouring Fe^{3+} site. In the limit of large J_H this is practically forbidden and the system will try to gain the superexchange energy, approximately $\sim \frac{t^2}{J_H}$, where t is the appropriate hopping integral between the relevant orbitals[2]. In contrast, in a ferromagnetic arrangement (figure 3(b)) the minority spin electron in Fe^{2+} can move to a neighbouring Fe^{3+} site without paying extra energy and the system gains kinetic energy (KE) in this process. From the above discussion, it is evident that when J_H is large the system will prefer to be in the ferromagnetic state rather than the antiferromagnetic one. If J_H is moderate then all these energy scales are comparable and the competition between kinetic energy, superexchange energy (SE) and J_H will decide the phase boundaries.

---

[2] Presence of doubly occupied e$_g$ orbitals in both initial and final states ensures that the intra-orbital Coulomb repulsion (U) contributes to the total energy in both states.
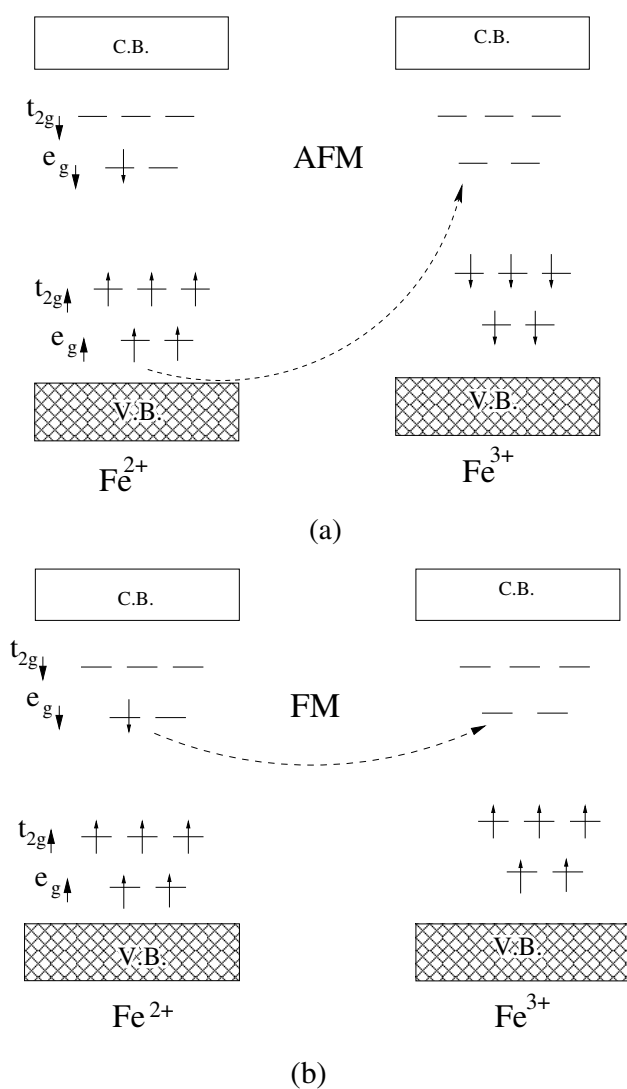
Figure 3. Electron hopping between Fe^{2+} and Fe^{3+} at neighbouring tetrahedral doped sites with (a) antiferromagnetic alignment of spins and (b) ferromagnetic alignment of spins.

It is useful to make a note at this point that the Fe^{2+} ion with three electrons in its e_g orbitals is likely to be Jahn–Teller (JT) active, i.e. the doubly occupied orbital stabilizes over the singly occupied one, whereas Fe^{3+} with two electrons in the two e_g orbitals is not JT active. In this case one can then work with only one e_g orbital for Fe^{2+} (the Jahn–Teller stabilized one) with electrons hopping through this orbital. The mechanism of magnetic exchange due to electron delocalization goes through without loss of generality as outlined above (with possible reduction in the overall e_g bandwidth, which can be scaled away). The third e_g electron in the Fe^{2+} site and the corresponding e_g orbital can be ignored. But as we will see in the following this single-orbital model is not sufficient to describe the case where all (or most of) the doped Fe are in an Fe^{2+} state. One has then to take into account both e_g orbitals and the hopping among them.

3.3. High Fe^{2+} concentration limit

Here we consider two neighbouring tetrahedral Fe ions, both in Fe^{2+} configuration. Since each of them has three electrons in their e_g orbitals, one e_g orbital is full and the other has one electron. Therefore the only way electrons can hop is via this half-filled orbital. In this case, there are several possibilities arising from the relative values of the JT stabilization energy (Δ) and the bandwidth (W) of the e_g bands ($\Delta \ll J_H$ for the system under consideration). Consider the situation when $\Delta > W$. In this case ferromagnetism is inhibited if the hopping matrix is diagonal. If, however, there exists off-diagonal hopping t^{12} (which, in general, depends on the orbitals involved and the symmetry of the lattice), then ferromagnetism could stabilize via a virtual hopping with a gain of ferromagnetic exchange energy $(t^{12})^2/\Delta$. This FM phase is not driven by KE as in the double-exchange mechanism. However, there is also a competing AFM phase that gains superexchange energy of order $t^2/(\Delta + J_H)$.

In the limit $\Delta < W$, the FM state is driven by the double-exchange mechanism as in the Fe^{2+}–Fe^{3+} mixed configuration. The FM state is stabilized by the KE of the e_g electrons since the superexchange energies are less than the KE. The underlying ground state, though, will be different when only diagonal hopping is allowed. In this case, in order to gain the KE, the Fe^{2+} ions will remain in a cooperative, staggered JT distorted arrangement which costs additional energy which depends on Δ and may not be stable if AFM superexchange energy is larger[3].

In figure 4 we show the situation arising in the case $\Delta = 0$ with the e_g orbitals in a cubic environment and nonzero overlap among them. One electron (either up or down) from the doubly occupied e_g orbital of Fe^{2+} on one site can always move to the singly occupied e_g orbital on the next Fe^{2+} site. In the case of antiferromagnetic alignment (shown in figure 4(a)) the hopping of an electron from one Fe^{2+} site to the next costs J_H amount of energy. The superexchange mechanism through virtual hopping is the only energy gain. In the ferromagnetic state (figure 4(b)), however, the initial and final states are degenerate and the system gains kinetic energy due to resonance. It is also evident that the physics for large Fe^{2+} concentration is different from the low Fe^{2+} concentration limit. In the low concentration limit, an effective single-orbital model captures the physical situation well, while in the high concentration limit, two bands are crucial for its understanding. This situation is somewhat reminiscent of the manganites where on the electron-doped side (hole concentration $x > 0.5$) the two e_g orbitals and the hopping between them play a crucial role in determining [17] the competition between the different magnetic phases, whereas on the hole-doped side ($x < 0.5$) a model with only the Jahn–Teller-stabilized single orbital is adequate.

4. Hamiltonian

Based on the above discussion we write down the following effective Hamiltonian for Fe-doped $ZnGa_2O_4$ assuming a cubic environment:

$$H = H_0 + H_{int}$$
$$H_0 = \sum_{\langle ij \rangle, \sigma, \alpha, \beta} t_{ij}^{\alpha\beta} c_{i\alpha\sigma}^\dagger c_{j\beta\sigma} - J_H \sum_i S_i \sigma_i + J_{AF} \sum_{\langle ij \rangle} S_i S_j \qquad (1)$$
$$H_{int} = U \sum_{i\alpha} n_{i\alpha\uparrow} n_{i\alpha\downarrow} + U' \sum_{i, \alpha \neq \beta} n_{i\alpha} n_{i\beta}.$$

Here we treat the t_{2g} electrons as localized and e_g as itinerant because the density of states (figure 1) clearly shows that the e_g down band is at the Fermi level, whereas the fully filled

---

[3] Such orbitally ordered states may be broken easily by defects in these disordered systems and long range transfer of charge carriers inhibited.

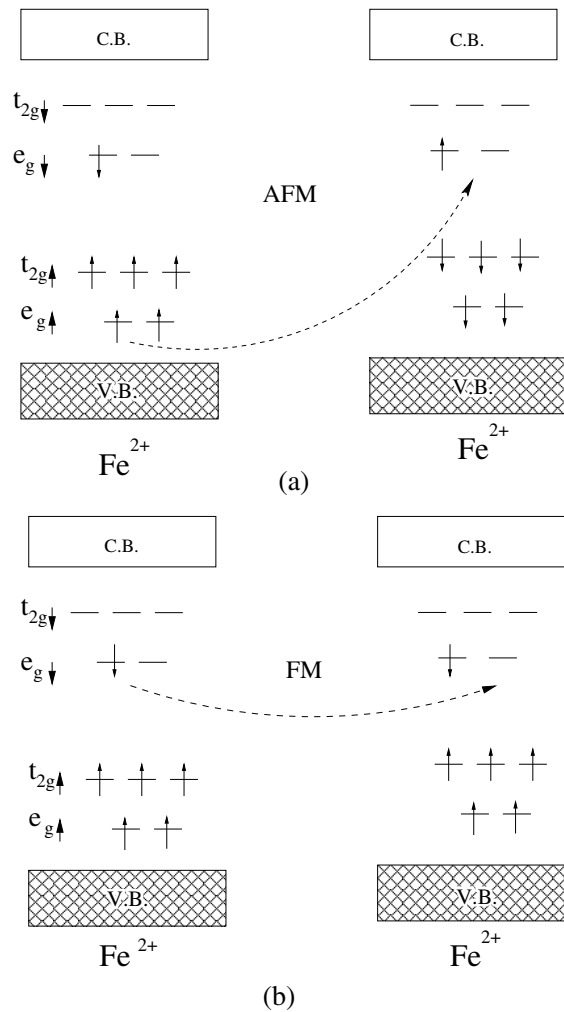**Figure 4.** Electron hopping in (a) antiferromagnetic phase and (b) ferromagnetic phase when both neighbouring doped tetrahedral sites are Fe^{2+}.

t_{2g} up band is well below. Electronic transport, therefore, involves the electrons in the e_g band primarily. The t_{2g} bands are well removed from the Fermi level and the e_g–t_{2g} overlap is negligibly small [19]. The t_{2g} electrons, under these conditions, provide a localized magnetic background, to which the itinerant e_g electrons are coupled through the Hund's exchange.

The first term in H_0 describes the kinetic energy with $t_{ij}^{\alpha\beta}$ being the anisotropic hopping integral between two e_g orbitals [19–21]. Here i and j are site indices and α, $\beta = 1, 2$ are e_g orbital indices. The second term is the Hund's coupling term between the localized t_{2g} spins and the itinerant e_g spins and the last term represents the antiferromagnetic superexchange coupling between neighbouring t_{2g} spins. The first and second terms in H_{int} define the onsite intra- and inter-orbital Coulomb repulsion with U and U' being the corresponding interaction strengths. In the half-filled situation when we have all Fe in Fe^{3+} states the ferromagnetic phase is blocked by the Pauli principle and an antiferromagnetic phase is favoured as we discussed above. The third term in H_0 representing the antiferromagnetic superexchange satisfies this limit.

First we discuss the model without considering the Coulomb correlation terms given by H_{int} (equation (1)). The correlation and their effects will be discussed later in detail. We treat the t_{2g} spin subsystem with a magnitude $3/2$ semiclassically, as is also the standard practice in the case of manganites [11]. We do not, however, make the further assumption prevalent in manganite and DMS literature, i.e. $J_H \to \infty$. Indeed, such an assumption would preclude the presence of an Fe^{2+} state. J_H in the foregoing is treated as a parameter and its value, as gleaned from the spin splitting observed in the band-structure calculations, is typically large (about 2.6 eV). Assuming an uncanted homogeneous ground state, we choose $S_i = S_0 \exp(i\mathbf{Q} \cdot \mathbf{r}_i)$ where $S_0 = 3/2$ and $\mathbf{Q} = (0, 0, 0)$ for the ferromagnetic phase and $\mathbf{Q} = (\pi, \pi, \pi)$ for the antiferromagnetic phase. With this choice the first two terms of the Hamiltonian H_0 (1) reduce to

$$H_1 = \sum \epsilon_k^{\alpha\beta} c_{k\alpha\sigma}^{\dagger} c_{k\beta\sigma} - J_H S_0 \sum c_{k\alpha\uparrow}^{\dagger} c_{k+Q\alpha\uparrow} + J_H S_0 \sum c_{k\alpha\downarrow}^{\dagger} c_{k+Q\alpha\downarrow} \qquad (2)$$

$$\epsilon_k^{11} = -2t(\cos k_x + \cos k_y)$$
$$\epsilon_k^{12} = \epsilon_k^{21} = -\frac{2}{\sqrt{3}}t(\cos k_x - \cos k_y) \qquad (3)$$
$$\epsilon_k^{22} = -\frac{2}{3}t(\cos k_x + \cos k_y) - \frac{8}{3}t \cos k_z.$$

Here equation (1) corresponds to $d_{x^2-y^2}$ and equation (2) to $d_{3z^2-r^2}$ orbital and t is the magnitude of the hopping integral between two neighbouring $d_{x^2-y^2}$ orbitals in the x, y direction. The superexchange contribution to the Hamiltonian is given by

$$E_{SE} = \frac{J_{AF} S_0^2}{2}(2 \cos \theta_{xy} + \cos \theta_z) \qquad (4)$$

where θ_{xy} and θ_z are the angles between neighbouring spins in the xy plane and in the z direction respectively. $\theta_{xy} = \theta_z = 0$ for the ferromagnetic phase and $\theta_{xy} = \theta_z = \pi$ in the antiferromagnetic phase. These two angles could be different from π or 0 in general and allow for canting.

We diagonalize the Hamiltonian (equation (2)) at each $\mathbf{k}$ point on a finite momentum grid and calculate the ground state energy for ferromagnetic and antiferromagnetic states in their uncanted spin configurations. The magnetic structure with minimum ground state energy is determined for each set of parameters (y, J_H and J_{AF}); the two e_g orbitals are taken to be degenerate currently ($\Delta = 0$). Here y is the e_g electron concentration, $y = 0.5$ corresponds to the limit where all Fe ions are in their Fe^{3+} state and $y = 0.75$ corresponds to all Fe in the Fe^{2+} state. In figure 5 we show the ground state phase diagram in the y–$J_H S_0/t$ plane with $J_{AF} S_0^2/t = 0.05^{Note\,4}$ as an illustration. However, this value of $J_{AF} S_0^2/t$ is varied in a wide range to obtain the phase diagram given in figure 6. In the above figure we see that at $y = 0.5$ where all Fe ions are in their Fe^{3+} state the system is antiferromagnetic at all values of the Hund's coupling J_H as we expected since the ferromagnetic state is blocked by the Pauli exclusion principle in this limit. As we increase the concentration of Fe^{2+}, the electron concentration increases in the down spin band, which can hop from site to site, and the system gains kinetic energy. Due to the competition, modulated by the value of J_H, between the kinetic energy which favours an FM configuration and superexchange energy which favours an AFM state, a ferromagnetic phase is indeed stabilized over the antiferromagnetic one for moderate to high concentration of Fe^{2+}. As the value of J_H is increased, the ferromagnetic phase becomes broader and at very large J_H the ferromagnetic region becomes almost independent of J_H.

In figure 6 we present the ground state phase diagram in the y–$J_{AF} S_0/t$ plane at a typical value of $J_H S_0/t = 25.0$ which is again estimated from the electronic structure

---

4 A typical value estimated from the Hund's coupling strength and the relevant bandwidth involved in the band-structure calculations.
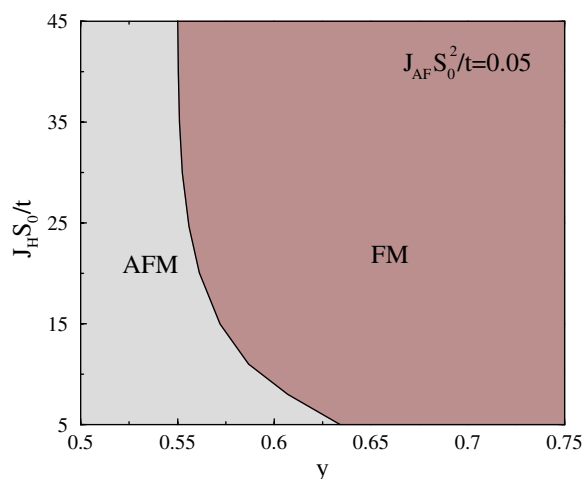
Figure 5. Ground state phase diagram of the Hamiltonian ($U = U' = 0$) in the y–$J_H S_0/t$ plane where y is the e_g electron concentration and with $J_{AF} S_0^2/t = 0.05$.
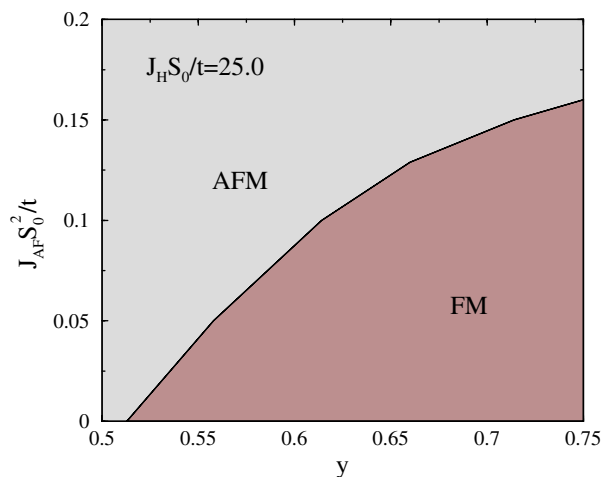

Figure 6. Phase diagram for Fe in a tetrahedral environment in the y–$J_{AF} S_0^2/t$ plane considering both e_g orbitals and the hopping among them in the model in the limit $U = U' = 0$.

calculation described above. Note that there exists a wide region in parameter space where the ferromagnetic phase is stabilized.

In the limit of non-degenerate e_g orbitals, we examine the situation for $J_H > \Delta > W$. As argued earlier, there exists the possibility of a ferromagnetic phase via double exchange here too in the region of mixed Fe^{2+}–Fe^{3+} shown in figure 7. In this case, the AFM state reappears as the Fe^{2+} concentration increases because of reduced effective hopping. The phase diagram is symmetric about $y = 0.625$ and the regions of stability of these phases are nearly independent of Δ for $\Delta > W$ as expected. The rather interesting possibilities involving orbital order have not been discussed here. The orbital order can be generated by the anisotropic hopping as well as the JT distortion. It can also be enhanced by the Coulomb correlations [17].
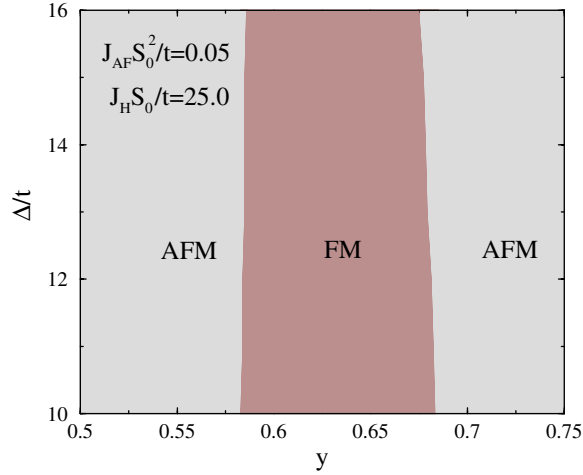
Figure 7. The ground state phase diagram for Fe in a tetrahedral environment in the y–Δ/t plane at a typical value of $J_H S_0/t = 25.0$ and $J_{AF} S_0^2/t = 0.05$.

5. Coulomb interaction

The onsite intra- and inter-orbital Coulomb interaction terms given by H_{int} (in equation (1)) are treated in the mean-field theory. Neglecting the fluctuation effects, we write $\hat{n}_{i1\sigma}\hat{n}_{i2\sigma'} = \langle\hat{n}_{1\sigma}\rangle\hat{n}_{i2\sigma'} + \langle\hat{n}_{2\sigma'}\rangle\hat{n}_{i1\sigma} - \langle\hat{n}_{1\sigma}\rangle\langle\hat{n}_{2\sigma'}\rangle$, the last term preventing double counting. The averages $\langle\hat{n}_{1\uparrow}\rangle$, $\langle\hat{n}_{1\downarrow}\rangle$, $\langle\hat{n}_{2\uparrow}\rangle$, and $\langle\hat{n}_{1\downarrow}\rangle$ are calculated from the eigenvectors iteratively through successive diagonalization of the Hamiltonian. Self-consistency has been achieved when all the averages $\langle\hat{n}_{i,\sigma,\alpha}\rangle$ and the ground state energy converge to within 0.01% or less.

It is well known [11, 22] that in the large J_H limit the Coulomb repulsion U between up and down spin electrons in the same orbital is ineffective in the mean-field theory. In this limit doubly occupied orbitals are energetically costly and generally avoided. However, in the case of Fe^{2+}, one of the e_g orbitals has to be doubly occupied. In this case, in the mean-field type argument, a replacement of J_H by $J_H + U$ in the doubly occupied orbitals takes care [22] of this repulsion. One then absorbs U in the value of J_H appropriately and does not consider it explicitly. In the following, therefore, we keep the value of U to be zero. There is, however, a strong effect of the inter-orbital Coulomb interaction (U') on the phase diagram as we discuss in what follows.

In figure 8 we present the effect of inter-orbital Coulomb interaction (U') on the ground state magnetic phase diagram for typical values of $J_H S_0/t$ and $J_{AF} S_0^2/t$, keeping $\Delta = 0$. As y increases, the FM phase appears as in the previous figures. At large U' and when almost all the Fe ions are in the +2 valence state, the AFM phase reappears at the right top corner of figure 8. In the presence of inter-orbital Coulomb interaction the energies in the high Fe^{2+} region are primarily dominated by localized exchange interactions. The competing interactions now have the energy scales $-\frac{t_{12}^2}{U'}$ and $-\frac{t_{22}^2}{J_H}$. In the limit $U' > J_H$ ($J_H + U$, if U is considered explicitly), the second term would provide extra gain in energy and the AFM phase should stabilize. A transition from FM $\rightarrow$ AFM will therefore occur as U' exceeds J_H for $y = 0.75$. As y reduces from 0.75, a larger U' is required for the transition, leading to the region of AFM at the top right-hand corner in figure 8 as shown.
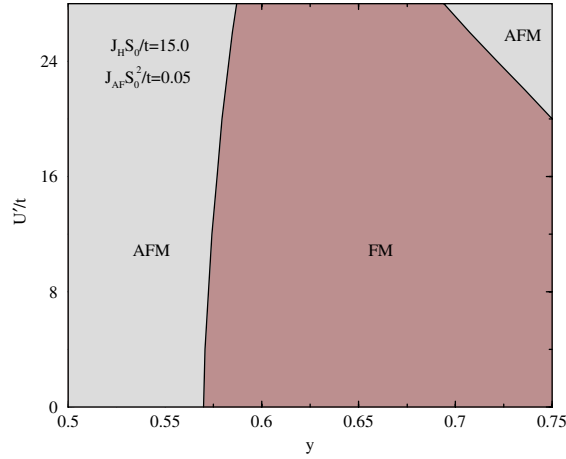
Figure 8. Phase diagram of the Hamiltonian for Fe in a tetrahedral environment showing the effect of U' (see equation (1)) on the ferromagnetic and antiferromagnetic phases.

6. Fe in octahedral position

So far we have investigated the case where the doped Fe ions are in the tetrahedral Zn positions of $ZnGa_2O_4$ with Fe^{2+} and Fe^{3+} valence states. Let us now examine the case when Fe is doped into octahedral Ga positions. In the octahedral crystal field the energy levels of Fe will be split into a triply degenerate set of t_{2g} levels and a doubly degenerate set of e_g levels. The t_{2g} levels in this case have lower energy than the e_g levels, contrary to the tetrahedral case. With this arrangement of orbitals, the extra (sixth) electron in Fe^{2+} will occupy the t_{2g} level. The preliminary band structure results with 25% Fe substitution in the Ga sites [18] corroborate this scenario. The overlap integrals between the t_{2g} orbitals are calculated as usual from the Slater–Koster integrals [19]. In this scenario, we consider the t_{2g} electron as itinerant for reasons similar to the ones discussed in the case of Fe in the tetrahedral position. We, therefore, use the overlap integrals between the t_{2g} orbitals in the kinetic energy term of Hamiltonian equation (2). We note at this point that in the spinel crystal structure of $ZnGa_2O_4$ these octahedral centres, occupied by the Ga atoms, are arranged in a tetrahedral fashion among themselves and hence are geometrically frustrated. We have not considered this geometrical frustration in the present calculation because the experimentally observed ratio of Fe to Ga is fairly small (1:6). The Fe atoms are assumed to be arranged in a cubic environment for the present calculation and hence there is no frustration.

In the kinetic energy term of the Hamiltonian given by equation (1) the orbital indices α and β now take the values 1, 2 and 3 which represent xy, yz and zx orbitals respectively. This Hamiltonian will reduce in **k**-space to the form of equation (2) as in the case of tetrahedral doping except from the fact that now $\epsilon_{\mathbf{k}}^{\alpha\beta}$ is a 3×3 matrix with the elements given by

$$
\begin{aligned}
\epsilon_k^{11} &= -2t'(\cos k_x + \cos k_y) \\
\epsilon_k^{22} &= -2t'(\cos k_y + \cos k_z) \\
\epsilon_k^{33} &= -2t'(\cos k_x + \cos k_z).
\end{aligned}
\tag{5}
$$

Here t' is the magnitude of the hopping integral between the neighbouring π-bonded xy orbitals in the x, y direction. Note that the inter-orbital overlaps turn out to be zero in this case [19]. Following similar procedures outlined in the tetrahedral case we calculate the
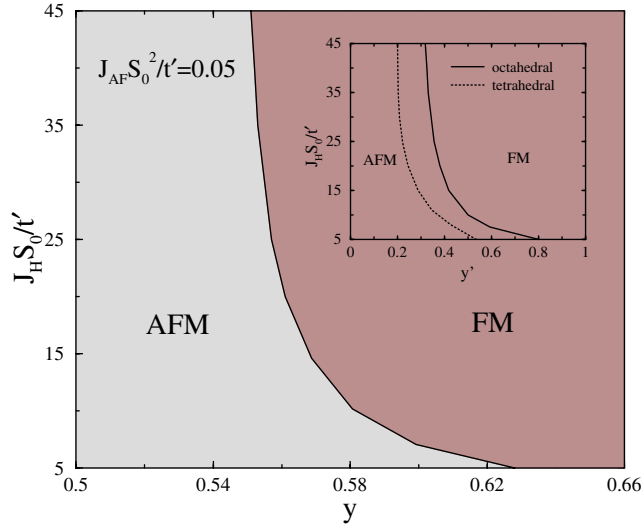
Figure 9. Phase diagram for the ground state of the Hamiltonian (with $U = U' = 0$) for Fe in an octahedral environment in the $y-J_H S_0/t'$ plane with $J_{AF}S_0^2/t' = 0.05$. In the inset we show the shift of the AFM–FM phase boundary compared to that of the tetrahedral case (the x-axis is rescaled such that $y' = 0$ corresponds to all Fe^{3+} and $y' = 1$ to all Fe^{2+} in order to make a comparison).

ground state magnetic phase diagram and observe that (as shown below) the ferromagnetic phase is stable in a wide range of parameter space in this case as well. However, we have not considered the Coulomb interactions (H_{int} in equation (1)) in the present calculation of the phase diagram.

In figure 9 we present the ground state phase diagram in the plane $y-J_H S_0/t'$ with a fixed value of $J_{AF}S_0^2/t' = 0.05$. The three t_{2g} orbitals have been taken as degenerate (i.e., $\Delta = 0$) and y is the electron concentration in the t_{2g} levels ranging from $y = 1/2$ (corresponding to all Fe^{3+}) to $y = 2/3$ (all Fe^{2+}, four electrons in t_{2g}). A comparison with the earlier phase diagram, for Fe in a tetrahedral position (figure 5), is shown in the inset. We observe a shift of the AFM–FM phase boundary towards higher concentration of Fe^{2+} in the octahedral case. The absence of off-diagonal hopping among the t_{2g} orbitals (equation (5)) reduces the effective KE gain in the double-exchange mechanism. This, in turn, makes the FM phase less stable compared to the tetrahedral case. The antiferromagnetic phase, therefore, stabilizes over a wider region in the phase diagram.

Nevertheless, we still observe a stable ferromagnetic phase in a moderate to high range of doping by Fe^{2+} ions. Finite JT splitting of t_{2g} orbitals may have interesting effects on the stability of the ferromagnetic phase in the high Fe^{2+} limit. Since the inter-orbital hopping is zero, even a small but finite JT splitting may induce a cooperative staggered JT distorted order of the Fe^{2+} ions in the ferromagnetic phase to maximize the KE. This would make the ferromagnetic phase increasingly destabilized against the AFM phase, depending on the value of Δ, as well as against defects and other impurities present in the system (see footnote 3). Coulomb correlations, particularly the inter-orbital Coulomb correlation (U'), is expected to have a strong effect in stabilizing the AFM phase in this case due to the reduced mobility of the carriers in the t_{2g} orbitals as argued above. Following the arguments in section 5, the AFM phase in the top right corner in figure 8 is expected to appear at a lower value of U' now.

7. Discussion

We observe from the above study of Fe doped $ZnGa_2O_4$ that ferromagnetism could result from a delicate competition between double exchange, favouring the FM spin order, and superexchange, favouring AFM order, when both Fe^{2+} and Fe^{3+} valence states are present. Though the present experimental situation in this system does not make the limit of all Fe^{2+} in tetrahedral positions a very relevant one, there is nevertheless a rich underlying physics connected with the interplay between dominant Jahn–Teller, double-exchange and superexchange interactions in this limit. Finally, a special note is in order for the case where the doped Fe ions go to both tetrahedral and octahedral environments replacing Zn and Ga ions respectively. In this mixed situation, it is necessary to first find out the extended and localized states from a careful density functional calculation. As the e_g–t_{2g} orbital overlap is negligible, it could be possible that in the mixed situation the double-exchange mechanism would operate within the Fe ions that belong entirely to one kind of crystalline environment (i.e. either in the tetrahedral or in the octahedral positions), and hence only a fraction of the Fe that are doped into the system would take part in the ferromagnetic long range order [3]. However, the model is expected to work as long as there are mobile electrons coupled to a relatively localized spin background.

We have been discussing in this work the carrier-mediated ferromagnetism which is believed to explain the magnetic properties of various dilute magnetic semiconductors with available free charge carriers [13, 14]. For relatively localized systems with no free carriers other alternative mechanisms such as that of the bound magnetic polaron model have also been proposed [23, 24]. One such example is Ga(Mn)N, where it has been suggested that the Mn ions are in d^5 configuration plus a localized hole and this localized hole forms a singlet with a Mn d electron (Zhang–Rice polaron) which then moves through the Mn sublattice and mediates ferromagnetic order [25, 26].

The system we consider in this work is different from other III–IV or II–VI semiconductors in some respects. First of all the doping concentration (50% or 25%) is quite high compared to, for example, the 6% doping in Ga(Mn)N. Secondly there is a possibility of Fe having a mixed valence state of Fe^{2+}/Fe^{3+}. Thirdly the existence of two kinds of crystalline environment to which Fe can be doped is not present in the known DMS semiconductors.

DMS systems like Ga(Mn)As have indeed shown dependence of T_c on the so-called antisite defects. Long range order in DMS systems is known to show sensitivity to disorder as well. But in the present context, disorder (which we did not consider) may not be that crucial for the underlying mechanism of magnetism proposed. Unlike the usual DMS materials, the doping is fairly high to be in the impurity dominated regime. The disorder may affect the values of exchange interaction and electron mobility, thereby shifting the phase boundaries slightly, but the overall topology of the ground state phase diagram will remain unaffected. Therefore, we believe that, at least to a first approximation, effects of disorder could be neglected.

Finally, concerning the model (equation (1)), there are also very interesting issues related to it like the possibility of phase separation and canted spin structures, possible orbital ordering and low dimensional spin orders which have not been investigated here.

8. Conclusion

In conclusion, based on the band structure results we have presented an effective model for magnetism in Fe-doped $ZnGa_2O_4$ which predicts a stable ferromagnetic phase when both Fe^{2+} and Fe^{3+} valence states are present. If only Fe^{3+} is present—as reported in the Mossbauer spectroscopy [3]—it is not possible to get ferromagnetism via this model; an insulating AFM

state would have been the most likely ground state. As the system is not very dilute and the transition temperature is quite high, it is likely that ferromagnetism in this system is driven by the kinetic energy of mobile electrons via double exchange rather than interaction between localized impurities. A high degree of delocalization of the extra electron in Fe^{2+} could also explain the observation of only Fe^{3+} states in the Mossbauer experiments. More experiments are needed to be done in order to unambiguously detect the states of Fe in $ZnGa_2O_4$. A study of the ground states for a range of doping concentrations would be very useful. Photoemission experiments backed by detailed first principles calculations are also indispensable to delineate the relevant orbitals that participate in the double-exchange mechanism.

Acknowledgments

References

[1] Ohno H 1998 *Science* **281** 951
[2] See Dietl T, Ohno H, Matsukura F, Cibert J and Ferrand D 2000 *Science* **287** 1019 and references therein
[3] Risbud A S, Seshadri R, Ensling J and Felser C 2005 *J. Phys.: Condens. Matter* **17** 1003
[4] Szotek Z, Temmerman W M, Svane A, Petit L, Stocks G M and Winter H 2003 *Phys. Rev.* B **68** 054415
[5] Sampath S K and Cordaro F 1998 *J. Am. Ceram. Soc.* **81** 649
[6] Itoh S, Toki H, Sato Y, Morimoto K and Kishino T 1991 *J. Electrochem. Soc.* **138** 1509
[7] Sampath S K, Kanhere D G and Pandey R 1999 *J. Phys.: Condens. Matter* **11** 3635
    Lauer M 2004 unpublished
[8] Hahn Th (ed) 2002 *International Tables for Crystallography* (Dordrecht: Kluwer)
[9] Blaha P, Schwartz K, Madsen G K H, Kvasnicka D and Luitz J 2001 *WIEN2K, An Augmented Plane Wave+ Local Orbitals Program for Calculating Crystal Properties (Techn. University Wien, Austria, 2001)* ed K Schwarz (ISBN 3-9501031-1-2)
[10] Mahadevan P, Zunger A and Sarma D D 2004 *Phys. Rev. Lett.* **93** 177201
[11] Dagotto E, Hotta T and Moreo A 2001 *Phys. Rep.* **344** 1
[12] Sato K and Katayama-Yoshida H 2002 *Semicond. Sci. Technol.* **17** 367
[13] Dietl T 2002 *Semicond. Sci. Technol.* **17** 377
[14] Pearton S J *et al* 2004 *Semicond. Sci. Technol.* **19** R59
[15] Wierzbowska M, Sanchez-Portal D and Sanvito S 2004 *Phys. Rev.* B **70** 235209
[16] Chattopadhyay A, Das Sarma S and Millis A J 2001 *Phys. Rev. Lett.* **87** 227202
[17] Maitra T and Taraphder A 2002 *Europhys. Lett.* **59** 896
    Maitra T and Taraphder A 2003 *Phys. Rev.* B **68** 174416
[18] Pisani L 2005 private communication
[19] Slater J C and Koster G F 1954 *Phys. Rev.* **94** 1498
[20] Anderson P W 1959 *Phys. Rev.* **115** 2
[21] Kugel K I and Khomskii D I 1973 *Sov. Phys.—JETP* **37** 725
[22] Hotta T, Malvezzi A and Dagotto E 2000 *Phys. Rev.* B **62** 9432
[23] Berciu M and Bhatt R N 2001 *Phys. Rev. Lett.* **87** 108203
[24] Das Sarma S, Hwang E H and Kaminski A 2003 *Phys. Rev.* B **67** 155201
[25] Dietl T, Matsukura F and Ohno H 2002 *Phys. Rev.* B **66** 033203
[26] Filippetti A, Spaldin N A and Sanvito S 2003 *Preprint* cond-mat/0302178